Bulgarian Chemical Communications, Volume 50, Special Issue J (pp. 135–146) 2018

Surface chemical states of cellulose, chitin and chitosan studied by density functional theory and high-resolution photoelectron spectroscopy

K. L. Kostov[1,*], E. Belamie[2, 3], B. Alonso[2], T. Mineva[2]

[1] *Institute of General and Inorganic Chemistry, Bulgarian Academy of Sciences, 1113 Sofia, Bulgaria*
[2] *ICGM-MACS, UMR 5253 CNRS-ENSCM-UM, Institut Charles Gerhardt de Montpellier, 240, Avenue du Professeur Emile Jeanbrau, 34090 Montpellier cedex 5, France*
[3] *Ecole Pratique des Hautes Etudes, PSL Research University, 75014 Paris, France*

Received March, 2018; Revised April, 2018

A combined theoretical and experimental approach has been applied to study the 1s electron-energy surface properties of cellulose, chitin, synthesized chitin nanorods and chitosan using density functional theory and high-resolution photoelectron spectroscopy. This allows to reliably distinguish the contributions of surface hydrocarbon impurities in the photoelectron spectra and to examine in detail the chemical states of the polysaccharide surfaces. Although a stoichiometric structure is suggested for the cellulose surface as more likely, a mechanism for possible degradation of the surface including removal of the OH group bonded to glucose ring is also contemplated. The good agreement between theoretical and experimental results allows suggesting a chitosan-like structure for the surfaces of as-prepared chitin and of chitin nanorods. In addition to the dominant concentration of amino NH_2 groups on these surfaces, a small amount of acetyl amine NH_2COCH_3 groups is also observed on the as-prepared chitin. It is possible that protonated amino NH_3^+ functional groups instead of acetyl amine are present on the crystalline surface of chitin nanorods. The possible destructive role of X-ray radiation on the studied surfaces is also discussed.

Keywords: DFT, XPS, cellulose, chitin, chitosan.

1. INTRODUCTION

In the surface area of the solids, the bulk field equilibrium is disturbed, causing a modification of its structure, often accompanied by a change in the chemical state of the surface atoms. On the other hand, the solids interact with the environment through their surfaces, and this process also causes changes in their chemical state. Therefore, in order to understand the mechanism of this interaction, which is of utmost importance for the modern life, the knowledge of the surface chemical state stands out with great significance. Experimentally, the X-ray photoelectron spectroscopy (XPS) is an appropriate method for analyzing the changes in the electron-energy structure of surface atoms and hence their chemical state. Due to the small inelastic free paths of the photoemitted electrons in the order of several nanometers, this method provides chemical information mainly for the top surface atoms. However, due to the variety of chemical bonds involving surface atoms, as in the case of polysaccharide surfaces, the photoelectron spectral regions often show complex structures. Their interpretation requires the use of theoretical methods, among which the methods of density functional theory (DFT) are highlighted. This combined theoretical and experimental approach provides a thorough and reliable analysis of the chemical state of the surface atoms.

Objects of the present study are the surfaces of some polysaccharides (cellulose, chitin, chitosan) and the interest in them is dictated by their extremely wide practical applications (see for example refs. 1–3 and references therein). For example, mats of fibers can be used as technical papers or as textiles for medical applications. In the form of nanorods, crystalline cellulose and chitin possess self-assembly properties leading to interesting applications, notably in optics due to the birefringence of the cholesteric mesophases. These nano-objects can also be used as templates for porous materials with designed textures, very useful in heterogeneous catalysis. Because of these applications, the

* To whom all correspondence should be sent:
E-mail: klkostov@gmail.com

polysaccharides have been studied extensively, but we focus only on those studies concerning the electron-energy structure of surface atoms.

The previous XPS studies have resolved mainly three C 1s peak contributions [4–10] as the first peak at lowest binding energy is attributed to carbon atoms in C-C and C-N bonds, the second peak at higher energies has been assigned as carbons in C-O-C, C-OH and the highest binding-energy third peak is interpreted as due to O-C-O bonding [4, 11]. In our study we are able not only to give more detailed information but also, in some aspects, to give a new interpretation of the experimental results. It seems that in the analysis of the N 1s photoelectron region there is a better consensus in the literature. A lower binding energy has been measured for the amino NH_2 group of chitosan with respect to acetyl amine $NHCOCH_3$ of chitin [4, 5, 7, 11]. The energy difference between them varies within 1.0–1.5 eV. However, it is possible that this varying energy difference is due to the presence of a third chemical state of nitrogen, for example positively charged nitrogen [12–15].

The experimental O 1s photoelectron region of cellulose, chitin and chitosan is less informative showing a broad asymmetric peak which is often fitted with 2 or 3 peak contributions with ambiguous interpretationin the previous studies [4, 7, 9]. All contradictions and incompleteness in characterization of the surface electron structure of cellulose, chitin and chitosan motivate our present study. It uses a combined theoretical (DFT) and experimental (XPS) approach allowing reliable results to be obtained for the stoichiometry and the chemical state of the uppermost layers.

2. EXPERIMENTAL AND THEORETICAL DETAILS

2.1. Apparatus

The X-ray photoelectron experiments have been carried out on AXIS Supra electron spectrometer (Kratos Analytical Ltd., a Shimadzu Group Company) with base vacuum in the analysis chamber of ~10^{-9} mbar. The spectra have been recorded using a monochromatic Al K_α excitation radiation with photon energy of 1486.6 eV. The photoemitted electrons are separated, according to their kinetic energy, by a 180°-hemispherical analyser. The detection system is characterized by hybrid type (electrostatic and magnetic) lenses of the analyser, charge neutralizer operating with low-energy electrons. The used spot size aperture in front of the electrostatic lenses and the analyser pass energy of 20 eV determine an instrumental resolution of 0.54 eV (full width at half maximum (FWHM) of Ag $3d_{5/2}$ peak). However, for isolator samples, the actual resolution is ~0.9 eV (measured by the half-width of the narrowest C 1s peak of cellulose) due to the charging effect caused by the electron photoemission.

The peak positions and areas have been evaluated by a symmetrical Gaussian-Lorentzian curve fitting. The concentrations (in at.%) of the observed chemical elements were calculated by normalizing the areas of the corresponding photoelectron peaks to their relative sensitivity factors using the commercial software of the spectrometer. The accuracy of the binding energy determination is within ± 0.1 eV. The corresponding error in concentration determination is around 1 at.%.

2.2. Theoretical details

All the calculations were carried out with Density Functional Theory based computer program deMon2k [16] with the generalized gradient-corrected PW91 [17] approximation for the exchange-correlation functionals. Empirical dispersion term as implemented in deMon2k was introduced in the geometry optimization [18]. The atoms were described with the double-zeta quality basis sets [19]. The 3-units models of cellulose, chitin and chitosan (see below) were optimized at the same level of theory. The 1s binding energies of carbon and nitrogen were computed using the Slater Transition state approach [20], as generalized later on within DFT by Janak [21]. Following this approach, the binding energy, E_b, is computed from the negative of the orbital energy ε_{1s} occupied by n = 0.5 electron: $E_b(1s) = -\varepsilon_{1s}(n)$.

2.3. Energy calibration

In our previous studies [22–24] the reported XPS results have been obtained using a spectrometer wherein the ultra-high vacuum is achieved by diffusion pumps. The energy scale calibration has been performed by normalizing the C 1s line of adsorbed adventitious hydrocarbons to 284.6 eV (equal to C 1s energy after their adsorption on conductive silver surface). In the present study, oil-free vacuum pumps were used which minimizes the adsorption of such hydrocarbons and their eventual C 1s peak is screened from the intense peaks of C 1s complex structure of studied materials. In this case we used the results from theoretical considerations normalizing the calculated C 1s binding energies of carbons having similar chemical environments as those in a benzene ring to 285 eV. The calibration procedure is similar to that used in our previous study on some coumarin-containing compounds [25].

2.4. Materials

The cellulose sample was purchased from GE Healthcare (Whatman – Chromatography paper 4 Chr, Cat. No. 3004-614). Flakes of chitin provided by France Chitine (http://www.france-chitine.com) and chitosan (high molecular weight, Aldrich) have been also studied. These samples are called "as-prepared chitin" and "as-prepared chitosan", respectively.

The sample of compressed chitin nanorods has been prepared in the Charles Gerhardt Institute (CNRS, Montpellier, France). The average length and diameter of these chitin monocrystalline nanorods are around 260 nm and 3 nm, respectively. The synthesis procedure and the properties of chitin nanorods are described in refs. 26 and 27.

3. RESULTS AND DISCUSSION

3.1. Cellulose

The studied 3-units model (Fig. 1) is constructed based on the bulk structure of cellulose.

The calculated 1s binding energies of the central-unit atoms are shown in Table 1. As mentioned in sect. 2.3 the energy scale is calibrated by normalizing the C 1s core-level energy of C2 carbon atom to 285.0 eV. The C4 and C5 carbon atoms have very close binding energies of 286.47 and 286.50 eV, respectively. Therefore, they would give a common peak contribution to the C 1s photoelectron spectrum with an area twice as large as the individual contributions of the remaining carbon atoms. The energies for the C6 and C3 carbon atoms are around these values, respectively, of 286.64 and 286.28 eV. The lowest C 1s energy of 285.0 eV has been calculated for the C2 carbon atom bonded to two carbon atoms of the glucose ring. Its neighbor, the C1 carbon atom, which is chemically bonded to two oxygen atoms, is characterized by the highest binding energy of 287.75 eV. Therefore, in the cellulose unit, six carbon atoms in five different chemical environments can be identified with concentration ratio of 2:1:1:1:1. Also, four non-equivalent oxygen atoms exist in the structural unit: O1 linked two adjacent glucose rings, O2 from the glucose ring, O3 and O4 from both OH groups bonded to CH_2 group and to the carbon C3 from glucose ring, respectively. Their theoretically calculated O 1s binding energies are also shown in Table 1.

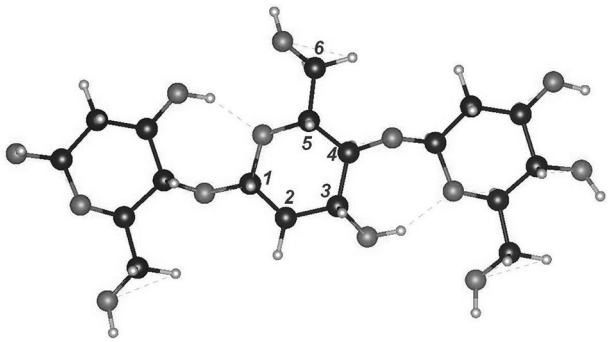

Fig. 1. (Color online) Structural model of cellulose including three units. The carbon and oxygen atoms are colored in green and red, respectively. The small circles with gray contour indicate hydrogen atoms. The hydrogen bonds are also marked with dash gray lines.

Using the areas of C 1s- and O 1s-peaks and their relative sensitivity factors in XPS the carbon-to-oxygen concentration ratio has been calculated to be C:O = 67:33 (at. %), which is different from the bulk stoichiometric ratio of 60:40 (assuming 6 carbon and 4 oxygen atoms in the cellulose unit). Note that the same concentration ratio of C:O = 67:33 (at.%) can be obtained assuming the presence of 6 carbon atoms and 3 oxygen atoms in the surface unit of the cellulose. On the other hand the calculated concentration ratio suggested an excess of carbon amount which can be explained with the presence of adsorbed hydrocarbon contaminations often measured on the polymer surfaces [28]. Therefore, we can consider two cases: (i) modification of the cellulose surface expressed in removing of one oxygen atom from the structural unit and (ii) the cellulose surface conserves its stoichiometry but there are adsorbed hydrocarbon contaminations.

(i) Modification of the cellulose surface

The approach to detecting eventual surface modification of cellulose involves deconvolution of experimental spectra using the theoretically calculated binding energies from Table 1 for a stoichiometric structural unit of cellulose and analysis of the resulting deviations from this stoichiometry.

The deconvolution of the experimental C 1s spectrum with five peaks with an area ratio equal to the stoichiometric carbon concentration ratio of 2:1:1:1:1 is shown in Fig. 2a.

If the individual fit peaks are interpreted in the manner shown in Table 1, the best match with the theoretical data is obtained. The energy differences (ΔE) between peak maxima of different C 1s fit-contributions and corresponding theoretically calculated values for the C1, C2, C4, C5 and C6 atoms are less than 0.1 eV (Table 1, modified surface). Note that this matching is within the experimental error (± 0.1 eV), which highlights the good agreement between the proposed interpretation and the experimental data for these carbon at-

Table 1. Theoretical 1s binding energies (in eV) of different carbon (C) and oxygen (O) atoms from the central unit of cellulose (see Fig. 1) compared to the experimental values derived by the deconvolutions of photoelectron spectra for modified and unmodified cellulose surface. ΔE is the difference between experimental and theoretical 1s energies

		Modified surface		Unmodified surface	
atom, electron-level	theory (eV)	exp (eV)	ΔE (eV)	exp (eV)	ΔE (eV)
C1	287.75	287.8	0.05	287.8	0.05
C2	285.00	285.0	0	285.0	0
C3	286.28	284.5	–1.78	286.3	0.02
C4	286.47	286.4	–0.07	286.5	0.03
C5	286.50	286.4	–0.10	286.5	0.00
C6	286.64	286.6	–0.04	286.7	0.06
other carbon		~289.0		~289.0	
O1 glyc. bond	535.06	532.8	–2.26	532.8	–2.26
O2 ring	534.96	532.8	–2.16	532.8	–2.16
O3 OH-CH2	535.53	533.3	–2.23	533.3	–2.23
O4 ring-OH	534.57			532.3	–2.27

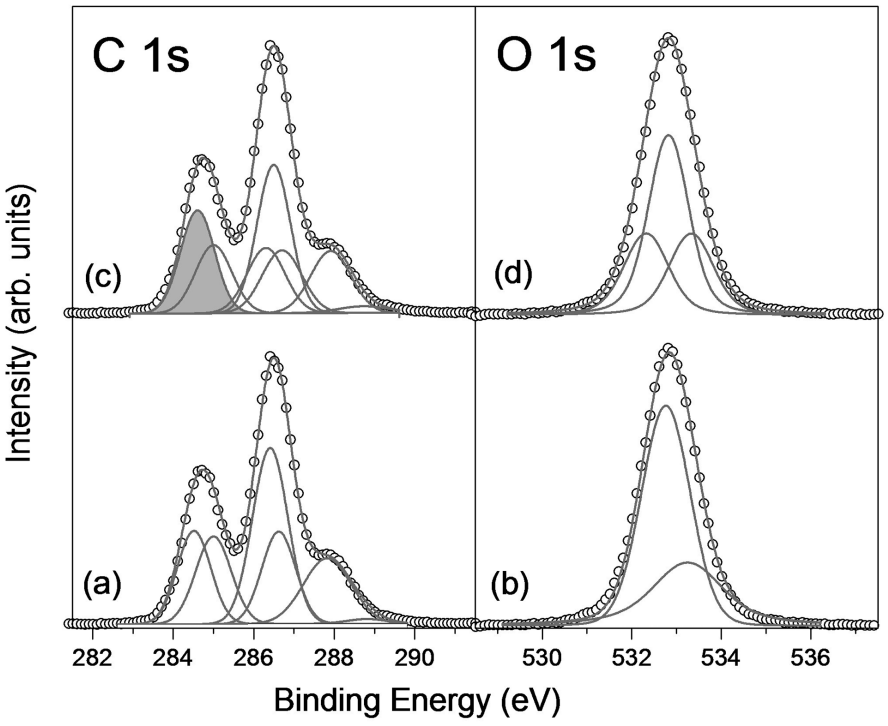

Fig. 2. (Color online) C 1s- and O 1s- photoelectron regions of cellulose (open circles) and their deconvolutions. Spectra (**a** and **b**) corresponds to modified surface by removing of the OH group bonded to glucose ring. Spectra (**c** and **d**) correspond to stoichiometric surface and contain a peak of surface contaminations (colored in gray). The peak contributions and their sum are marked in blue and red, respectively.

oms. However, there is a large exception concerning the carbon atom C3 from the cellulose structural unit (Fig. 1). The deconvolution suggests that its C 1s binding energy should be 284.5 eV instead of 286.3 eV calculated theoretically (Table 1). The difference between the theoretical and experimental C 1s energies of C3 carbon is 1.78 eV, which is too large to be explained by the error of both theoretical and experimental approaches. Most likely, the explanation is in the sensitivity of the experimental method to the upper surface atoms of the cellulose, whereas the theoretical model is based on the cellulose bulk structure. Therefore a large C 1s chemical shift can be proposed for surface C3 carbon atom with respect to its bulk bonding and respectively a chemical modification of this surface atom can be suggested.

As it was mentioned above the experimental concentration ratio has been calculated to be C:O = 67:33 (at.%), which could correspond to the presence of 6 carbon atoms and 3 oxygen atoms in the surface unit of the cellulose. Indeed, the removal of an oxygen atom (respectively the OH group) attached to the C 3 carbon atom would cause a large chemical shift of its C 1s binding energy. In this case the C3 carbon atom could have a similar chemical state like C2 and a close C 1s binding energy, respectively.

The hypothesis for cellulose surface modification connected with the absence of OH group bonded to surface C3 carbon can be proved considering the O 1s core-level results. In contrast to the C 1s region the O 1s spectrum is characterized by a single symmetrical peak at 532.8 eV with half-width (FWHM) of 1.3 eV (Fig. 2b). This makes the interpretation of the chemical states of the individual oxygen atoms in cellulose unit difficult and it can be done only with theoretical help. In Table 1 the calculated O 1s binding energies of the four non-equivalent oxygen atoms from the stoichiometric cellulose unit are shown. It can be seen that the oxygen atoms of the glucose ring and those connecting two adjacent rings have almost the same binding energies of ~ 535.0 eV. Between both hydroxyl groups bonded to the glucose ring and to the C6 carbon atom, respectively, there is an O 1s chemical shift of 1 eV. By using these values, the experimental O 1s spectrum may be fitted with two contributions (2 oxygen atoms related to glucose ring and one oxygen atom from OH group bonded to C6 carbon) with area ratio of 2:1 according the hypothesis of absence of the OH group bound to the glucose ring. The deconvolution may be considered as satisfactory if a relatively broad fit peak of the OH group with a larger Lorenz contribution is allowed (Fig. 2b).

The energy difference of about 2.2 eV between theoretical and experimental fit values exist (Table 1). This value can be considered as a systematical error related to the energy scale calibration for the different carbon and oxygen atoms. In our study we use for the calibration of O 1s energy the normalization of C 1s binding energy of C5 carbon atom to 285 eV (Table 1). A similar systematical error has been also observed in our previous study of coumarin-containing compounds [25].

(ii) Stoichiometric cellulose surface with adsorbed hydrocarbon contaminations

However, there are indications for another interpretation of the C 1s results that could be more realistic since it is difficult to explain the reasons for removing the OH group from the surface structure of the cellulose. In sect. 2.3 we noted that the hydrocarbon contaminations (CH_x) are characterized with C 1s binding energy at 284.6 eV and this value can be used for the energy calibration of photoelectron measurements of nonconductive materials. Also, in the next section 3.2 such a peak of surface contaminations has been detected for chitin and chitosan surfaces. In this connection, the presence of such impurities can also be assumed on the surface of the cellulose. To prove this hypothesis, a new deconvolution of the C1s spectrum has been made using 6 peak contributions: one peak of eventual hydrocarbon impurities at 284.6 eV and 5 other peak contributions of stoichiometric cellulose unit following the theoretically calculated binding energies and the stoichiometric ratio of the areas of these peaks in a 2:1:1:1:1 ratio (Fig. 2c). Within this hypothesis, as shown in Table 1 (unmodified surface), the agreement between the theoretical and experimental data is very good. Also the symmetrical O 1s experimental spectrum can be fitted very well using 3 contributions with area ratio of 1:1:2 (Fig. 2d). These contributions correspond to the four oxygen atoms in the cellulose unit including those from both OH unit groups (O3 and O4) with binding energy difference of 1 eV as mentioned above and also two oxygen atoms (O1 and O2, related to the glucose ring) with equal O 1s-energies at 532.8 eV. Therefore, the area of the last contribution is twice as large as the other peak contributions. The agreement with the theoretically calculated binding energies is again very good if the systematical error of 2.2 eV of the energy scale is neglected (Table. 1).

Also, ignoring the fit peak of proposed contaminations at 284.6 eV, the calculated ratio of carbon and oxygen concentrations of 62:38 is close to the cellulose stoichiometry (60:40). Hence, this second hypothesis (called “unmodified surface”) characterizes the cellulose surface as stoichiometric but also containing a certain amount of adsorbed hydrocarbon impurities. The first hypothesis (modified cellulose surface) implies some degree of degradation

of the cellulose chains involving the cleavage of OH groups linked to the glucose ring. Regardless of the realistic nature of this hypothesis, it definitely gives information about a possible mechanism (or at least as a mechanism step) for the degradation of the cellulose surface, which, eventually, could be one of the reasons for the existence of the detected hydrocarbon impurities.

Nevertheless 6 non-equivalent carbon atoms and 4 non-equivalent oxygen atoms exist in the cellulose unit, in the previous studies [29, 30] only two of the measured C 1s-peaks at 286.7 and 288.1 eV are attributed to cellulose carbons in –CH(OH) and –O-CH-O-, respectively. The measured third peak, in ref. 28, at 284.6 eV has been attributed only to contaminations. Two O 1s-peaks have been suggested to exist at 532.9 and 533.5 eV connected to oxygen atoms in -O- and -OH bonding, respectively [29, 30]. In comparison to these studies we are able to give significant more detailed description on the chemical states of different carbon and oxygen atoms and their C 1s- and O 1s-binding energies (Table 1).

For the complete characterization of the C 1s photoelectron spectra, the presence of a low intensity peak at about 289 eV, characteristic of carboxylic carbon, should be noted (Fig. 2a, c). Its negligible amount is an indication for the high quality of the cellulose surface and also for low influence of the X-ray radiation (and also electron exposure from the charge neutralization gun) on cellulose stoichiometry [28].

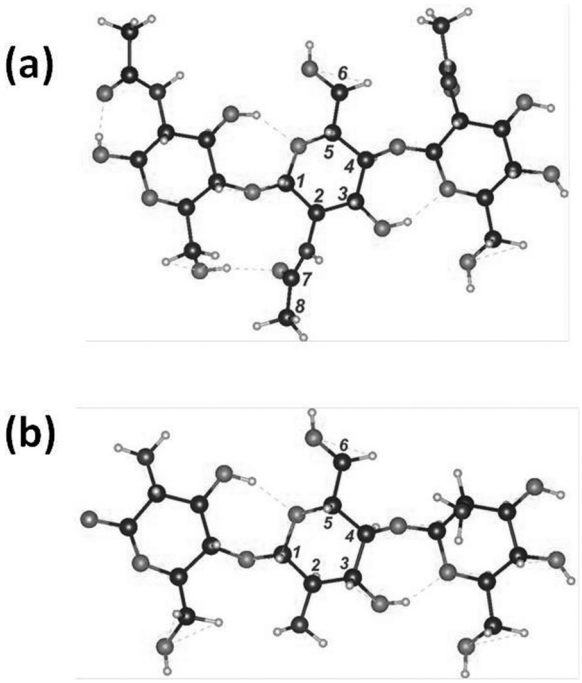

Fig. 3. (Color online) Structural models including 3-units of chitin (**a**) and chitosan (**b**). The carbon and oxygen atoms are colored in green and red, respectively. Blue-colored circles denote nitrogen atoms. The small circles with gray contour indicate hydrogen atoms and the hydrogen bonds are marked with dash gray lines.

3.2. Chitin and chitosan

Again, as for cellulose, three-unit structural models of chitin and chitosan have been analyzed theoretically (Fig. 3a and 3b) based on earlier experimental studies (for example refs. 5 and 31). The main difference between both models is the different functional groups connected to the C2 carbon atom: acetyl amine $NHCOCH_3$ for chitin (Fig. 3a) and amino NH_2 group for chitosan (Fig. 3b), respectively.

Now, the C2 atoms have quite different chemical environments than the cellulose C2 carbon atom, which C 1s binding energy has been chosen for the experimental energy-scale calibration (sect. 3.1). Therefore, in the case of chitin and chitosan, another carbon atom should be chosen for energy calibration. Considering the structural models of the polysaccharides (Fig. 1 and Fig. 3), the C5 carbon atom can be proposed as a suitable candidate because it has a similar chemical environment in all three studied compounds. Its calibrated theoretical binding energy for cellulose is at 286.5 eV (Table 1). This value is used to calibrate the calculated C 1s binding-energies for chitin and chitosan. The resulting energies are shown in Table 2.

In contrast to cellulose, determination of the corresponding C 1s energies for different carbon atoms of as-prepared chitin, chitin nanorods and as-prepared chitosan is quite difficult because significant deviations from ideal stoichiometry are seen mainly in the contents of carbon atoms. Evidence for this is found in the concentrations of the surface atoms (Table 3).

Also the photoelectron spectra show a complex structure in which individual peak contributions are not as clearly resolved as in the case of cellulose (Fig. 4).

From Table 3 it can be concluded that the contents of nitrogen and oxygen atoms in the case of as-prepared chitosan and chitin nanorods are close to those in the ideal chitosan unit structure. Also, excluding the intense peak at about 284.5 eV, the remainder of the C 1s spectra can be very well matched to the chitosan spectrum and its deconvolutions with chitosan-like contributions give a good agreement with the theoretically calculated binding energies (Table 2). Therefore it seems that the sur-

Table 2. Theoretical 1s binding energies (in eV) of different carbon (C), nitrogen (N) and oxygen (O) atoms from the central units of chitin and chitosan (see Fig. 3) compared to the experimental values for as-prepared chitin, chitin nanorods and as-prepared chitosan derived by the deconvolutions of the photoelectron spectra

Atom	Chitin			Chitosan	
	theory (eV)	as-prepared exp (eV)	nanorods exp (eV)	theory (eV)	exp (eV)
C1	287.31	287.7	287.8	287.36	287. 8
C2	286.67	286.1	286.1	285.43	285.2
C3	286.36	286.1	286.1	286.06	286.1
C4	285.36	285.4	285.4	286.37	286.1
C5	286.50	286.7	286.5	286.50	286.5
C6	286.49	286.7	286.5	286.50	286.5
C7	288.02	288.7	288.5		
C8	285.11	285.3	285.4		
other carbons		284.4	284.5		284.5
N $NHCOCH_3$	401.00	401.0	401.5?		
N NH_3^+			401.5?		
N $-NH_2$		399.7	399.6	399.90	399.3
O1 glyc. bond	534.85	532.8	532.7	535.30	532.7
O2 ring	534.17	532.3	532.1	534.80	532.0
O3 OH-CH2	535.73	532.8	532.7	535.38	532.7
O4 ring-OH	535.47	531.6	531.6	534.52	531.7
O5 $NHCOCH_3$	534.02				

Table 3. Concentrations of carbon, nitrogen and oxygen atoms (in at.%) for as-prepared chitin, chitin nanorods and as-prepared chitosan. The experimental values are compared with the ideal concentrations (stoichiometry) and also with the number of the carbon-, nitrogen- and oxygen-atoms in one structural unit of the studied compounds shown below the atomic percentages

		Carbon	Nitrogen	Oxygen
Chitin	exp.	66.5 11.3	5.9 1	27.6 4.7
	ideal	57.1 8	7.1 1	35.7 5
Chitin nanorods	exp.	65.8 9.7	6.8 1	27.4 4.0
	ideal	57.1 8	7.1 1	35.7 5
Chitosan	exp.	73.4 14.1	5.2 1	21.4 4.1
	ideal	54.5 6	9.1 1	36.4 4

face chemical states of chitosan and chitin nanorods are very similar. Note that the individual fit contributions have areas corresponding to the ideal chitosan stoichiometry. For example, each component of the two intensive contributions at about 286.5 and 286.1 eV in Fig. 4c corresponds to two carbon atoms (with close theoretically calculated C 1s binding energies) of the chitosan unit cell. Accordingly, their areas are twice as large as those of the other chitosan components (Fig. 4c). .

As mentioned above, the intense peak contribution at 284. 5 eV is an exception to this ideal chitosan-like structure. Note that the C 1s binding energy of adventitious hydrocarbons adsorbed on silver surface is measured at 284.6 eV (see sect. 2.3). Also, a similar binding energy is received for the surface C2 carbon atom of cellulose (Fig. 4d) existing in CH_2 group. Therefore, the lowest energy peak in Fig. 4 can be attributed to CH_x hydrocarbon

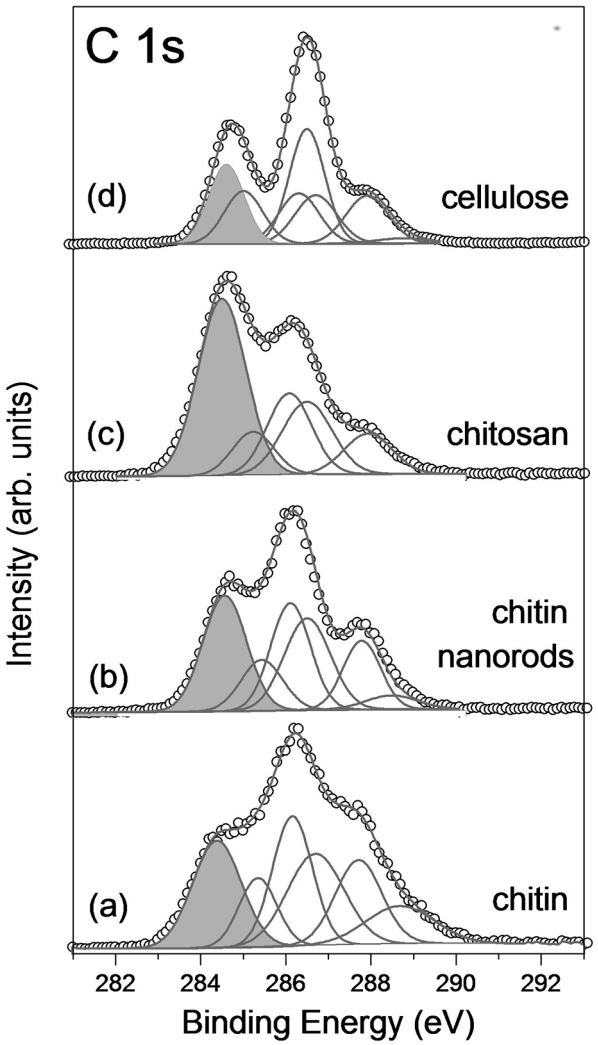

Fig. 4. (Color online) C 1s- photoelectron spectra (open circles) of as-prepared chitin (**a**), chitin nanorods (**b**), as-prepared chitosan (**c**) compared to the spectrum of cellulose (**d**). The peak contributions and their sum are colored in blue and red, respectively. The intense peak contribution corresponding to hydrocarbon contaminations is colored in gray.

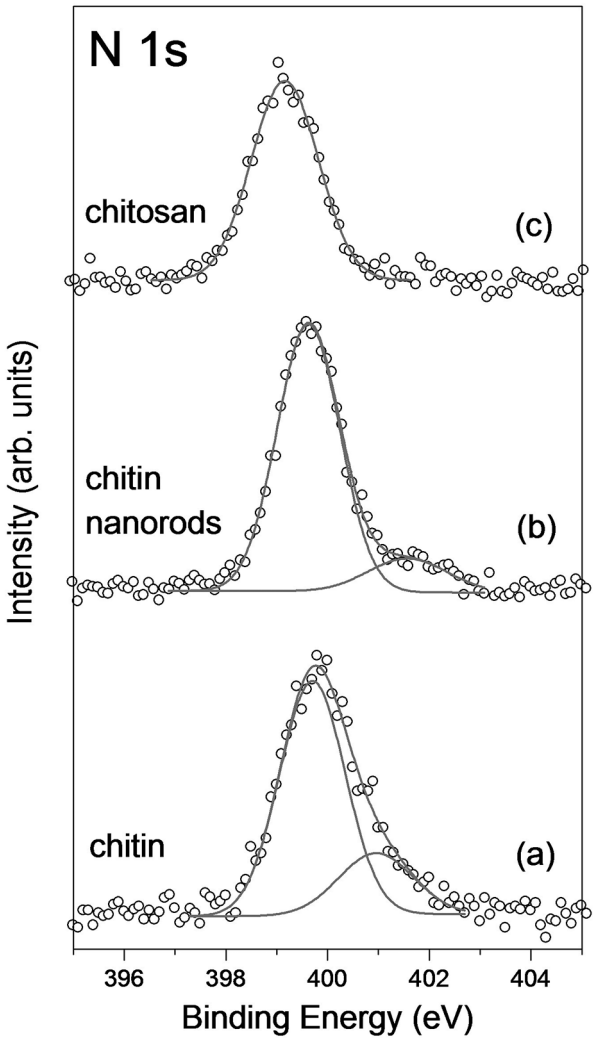

Fig. 5. (Color online) N 1s- photoelectron spectra (open circles) of chitin (**a**), chitin nanorods (**b**) and chitosan (**c**). The peak contributions and their sum are colored in blue and red, respectively.

groups adsorbed on the surfaces of the studied materials.

Another exception to the ideal chitosan structure is the additional peak at the highest binding energy of 288.5 eV, which appears in the deconvolution of the as-prepared chitin (Fig. 4a) and to a lesser extent in chitin nanorods spectra (Fig. 4b). According to the theoretical considerations this peak can be attributed to C 1s binding energy of C8 carbon atoms from acetyl amine $NHCOCH_3$ group characteristic for the ideal chitin structure (Table 2). Consequently, surface areas with a chitin-like structure could also provide contributions to the C 1s spectra. This can also reflect the deviations of area ratio of the other fit peaks from the stoichiometric area ratio of chitosan, which is observed in Fig. 4a and 4b.

The presence of nitrogen in two different chemical states on the surfaces of as-prepared chitin and of compressed chitin nanorods is evident from their N 1s photoelectron spectra (Fig. 5).

A single symmetric N 1s peak at 399.3 eV has been observed for the as-prepared chitosan attributed to nitrogen atom in NH_2 group in agreement with the theoretical calculations (Table 2). For as-prepared chitin and chitin nanorods, an additional less intense peak has been observed at 401.0 and 401.5 eV, respectively (Fig. 5a and 5b). According to the theoretical predictions in Table 2, the higher

binding energy of this peak implies the presence of nitrogen atoms from the acetyl amine $NHCOCH_3$ group. However, the significantly more intense N 1s peaks at about 399.6 eV indicate the dominant presence of amino NH_2 groups in comparison to acetyl amine concentration on both chitin surfaces.

The N 1s results are in agreement with the study of Jiang *et al.* [5] where beside the low- binding energy of nitrogen in NH_2 group another chemical state is found shifted by 2 eV to the higher binding energy. On the other hand, for as-prepared chitin and chitin nanorods an energy difference of 0.5 eV exists between N 1s binding energies for suggested acetyl amine $NHCOCH_3$ groups on both surfaces (Table 2). This energy difference is difficult to be explained because the surfaces show very similar electron-energy structure. It is possible that instead of (or in addition to) acetyl amine group there is more positively charged nitrogen on the surface of chitin nanorods, for example in NH_3^+ configuration. Confirmation for such an interpretation can be found in the N 1s spectrum of adsorbed alanine, where two peaks are observed at 401.8 and 401.3 eV related to NH_3^+ and NH_2 groups, respectively [32]. Note that the energy difference between both nitrogen chemical states is exactly 0.5 eV as in the case of as-prepared chitin and chitin nanorods.

In the structural unit of the chitosan-like surface there are 4 oxygen atoms in different chemical environments: in OH-group bonded to CH_2-functional group, into the glucose ring, between two glucose rings, in OH-group bonded to a carbon of this ring. However the experimental O 1s spectra of the three polysaccharides represent wide peaks with a clear broadening at low binding-energy side (Fig. 6). Together with the above discussed similarities of C 1s regions they indicate similar chemical states of the studied surfaces having most probably a chitosan-like structure.

The detailed contributions of the chemically different oxygen atoms to the photoelectron O 1s spectra can be understood only with the theoretical help. The calculated O 1s binding energies are shown in Table 2 for chitin and chitosan units as a better agreement with the experimental data has been found for the chitosan values. The lowest binding energy at 531.6 eV is obtained for the oxygen atoms of an OH group attached to the glucose ring. This is in agreement with the study of Jiang *et al.* [5] but in contrast to other XPS studies [4, 7, 9] where it has been assumed a lower O 1s binding energy for the oxygen atoms in ring-O-ring than the O 1s energy in OH-C configurations.

The differences between O 1s details of chitosan-like and cellulose surfaces indicate the influence of the amino group. Only the oxygen atom linked two adjacent glucose rings conserves its O 1s binding energy (Table 1 and 2) whereas a chemical shift of ~0.5 eV is observed for the other oxygens in comparison to the cellulose results. The largest chemical shift of 0.7 eV is found for the OH group bonded to the glucose ring.

Similar to the cellulose surface, a large chemical shift of 1.2 eV is observed between binding energies of both OH-groups bonded to carbon from CH_2 and bonded to the glucose ring, respectively (see Table 1 and Table 2). This is in contrast to the literature where the O 1s contributions of both chemically non-equivalent OH groups from the polysaccharide unit have been assigned to one peak at higher binding energies [4, 7, 9, 15].

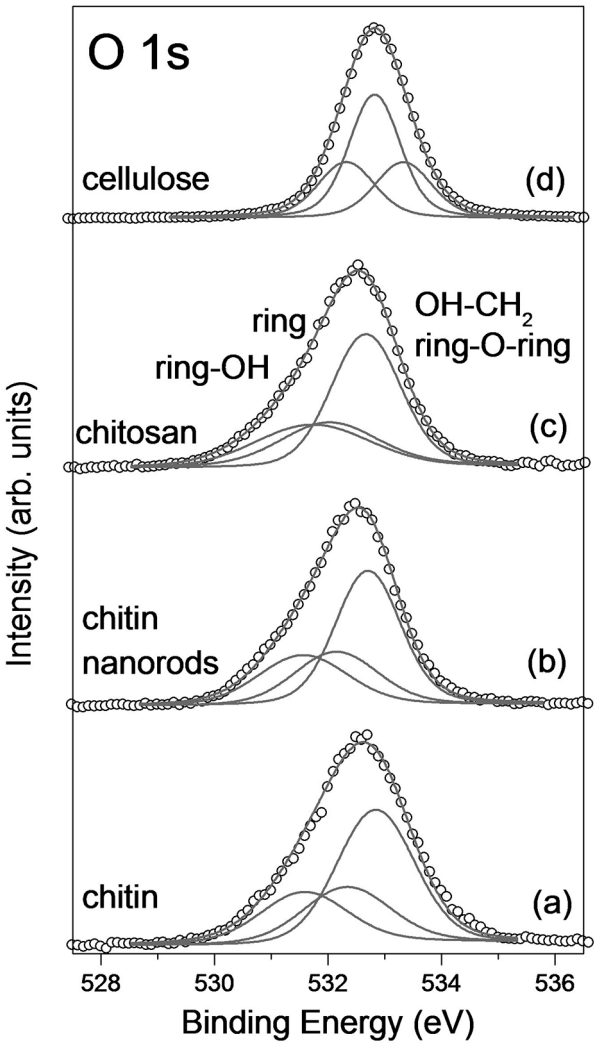

Fig. 6. (Color online) O 1s- photoelectron spectra (open circles) of as-prepared chitin (**a**), chitin nanorods (**b**) and as-prepared chitosan (**c**) compared to the spectrum of cellulose (**d**). The peak contributions and their sum are colored in blue and red, respectively. The peak interpretation is indicated on the figure.

From the discussed results it can be seen that their chemical states of chitin surfaces differ from those in their volume. Also, large amounts of surface hydrocarbon contaminations have been measured. The question remains to what extent these surface modifications are caused by the influence of the experimental method, i.e. the X-ray radiation and electron exposure. Such influences may be significant in the case of organic substances. For example, in the XPS study of brewer's yeast strains [33], their degradation during experiments have been observed reflected in an increase in surface hydrocarbon contaminations and decrease in the relative surface concentrations of nitrogen and oxygen atoms. Although in this sensitive case, the degradation cannot mask the real properties of the materials, the influence of the X-ray radiation should be carefully examined [28]. In fact, the eventual modifications can be caused not only by X-ray radiation, but mainly by the inelastic scattering of emitted photoelectrons as shown by Graham *et al.* studying organic layers [34].

We have investigated this eventual effect by varying the flux of X-ray radiation, respectively the X-ray power. Our measurements have been carried out at low powers (75–150 W) where no changes in the spectra with the analysis time have been observed. At high X-ray source power of 300–450 W a slight change of the analyzing-area color is visible accompanied with the small intensity increase of the low binding energy peak at 284.5 eV, which is interpreted as due to surface hydrocarbon contaminations. However, even in this case the other main features of the surface spectra are not affected.

4. CONCLUSIONS

The results show that, despite the high resolution and signal strength of the experimental method XPS, reliable analysis is achieved only in combination with theoretical modeling. This approach allows both the concrete understanding of the experimental C 1s-, O 1s-, N 1s- photoelectron spectra, but also the processes leading to the surface chemical modifications.

In the case of cellulose, its C 1s- and O 1s-photoelectron spectra can be described in details following the theoretical interpretation based on the stoichiometry preservation in the surface layers. The comparison with the theoretical calculations allows identifying a peak of surface hydrocarbon contaminations in the complex C 1s spectrum. Moreover, it allows suggesting a mechanism for degradation of the surface related to removal of surface OH group bonded to the glucose ring. This is accompanied by a decrease in C 1s binding energy of the corresponding carbon atom from the ring to 284.5 eV, exactly at the energy position characteristic for the hydrocarbon contaminations. Therefore, the removal of the OH group could be considered as a step in the process of creating surface hydrocarbon impurities.

An intense C 1s peak at 284.5 eV, attributed to surface hydrocarbon contaminations, is also observed for the studied chitin- and chitosan surfaces. Excluding this peak, the rest of their spectra can be well matched to the chitosan spectrum based on the theoretical predictions. According to these proposed chitosan-like structure of the chitin surfaces, the XPS results show a dominant concentration of surface amino NH_2 group. Additionally a small amount of acetyl amine NH_2COCH_3 is also found. For the monocrystalline surface of chitin nanorods, the presence of protonated nitrogen configuration, for example NH_3^+, is not excluded.

The experimental cellulose-, chitin- and chitosan-O 1s spectra can be very well described using theoretically calculated binding energies for the stoichiometric structural unit of corresponding polysaccharide. In contrast to the previous studies a large chemical shift of 1.0–1.2 eV is observed between O 1s energies for both non-equivalent OH-groups from the functional groups of all three polysaccharides.

Within the X-ray fluxes used (X-ray source power of 75–150 W), no spectra change is observed showing that the observed surface chemical modifications of the studied polysaccharides cannot be caused by the X-ray exposure during the experimental analysis.

Acknowledgements: *The authors acknowledge the financial support by the bilateral Bulgarian-French RILA 01/2-21.06.2013 Project. The calculations were performed at the HPC resources of TGCC-CURIE under the allocation x2017087369 made by GENCI (Grand Equipement National de Calcul Intensif).*

REFERENCES

1. M. N. V. Ravi Kumar, *React. Funct. Polymers*, **46**, 1 (2000).
2. A. Bhatnagar, M. Sillanpää, *Adv. Coll. Interface Science*., **152** , 26 (2009).
3. R. Jayakumar, M. Prabaharan, S. V. Nair, S. Tokura, H. Tamura, N. Selvamurugan, *Progress in Materials Science*, **55**, 675 (2010).
4. L. J. Matienzo, S. K. Winnacker, *Macromol. Mater. Eng.*, **287**, 871 (2002).
5. H. Jiang, J. Liang, J. T. Grant, W. Su, T. J. Bunning, T. M. Cooper, W. W. Adams, *Macromol. Chem. Phys.*, **198**, 1561 (1997).

6. Y. Wang, S. Yin, L. Ren, L. Zhao, *Biomed. Mater.*, **4**, 035003 (2009).
7. J. Chen, K. Nan, S. Yin, Y. Wang, T. Wu, Q. Zhang, *Colloids and Surfaces B: Biointerfaces*, **81**, 640 (2010).
8. A. Di Giuseppe, M. Crucianelli, M. Passacantando, S. Nisi, R. Saladino, *J. Catal*., **276**, 412 (2010).
9. J. Li, J.-F. Revol, R. H. Marchessault, *J. Coll. Interface Science*, **192**, 447 (1997).
10. J. Wang, Z. Wang, J. Li, B. Wang, J. Liu, P. Chen, M. Miao, Q. Gu, *Carbohydrate Polymers*, **87**, 784 (2012).
11. M. C. Burrell, M. D. Butts, D. Derr, S. Genovese, R. J. Perry, *Appl. Surface Sci.*, **227**, 1 (2004).
12. G. Lawrie, I. Keen, B. Drew, A. Chandler-Temple, L. Rintoul, P. Fredericks, L. Grundahl, *Biomacromolecules*, **8**, 2533 (2007).
13. F. Chen, Z. Shi, K. G. Neoh, E. T. Kang, *Biotech. Bioeng*., **104**, 30 (2009).
14. Y. Liua, X.-W. Shi, E. Kim, L. M. Robinson, C. K. Nye, R. Ghodssi, G. W. Rubloff, W. E. Bentleye, G. F. Payne, *Carbohydrate Polymers*, **84**, 704 (2011).
15. H. Maachou, M. J. Genet, D. Aliouche, C. C. Dupont-Gillain, P. G. Rouxhet, *Surf. Interface Anal*., **45**, 1088 (2013).
16. G. Geudtner, P. Calaminici, J. Carmona-Espíndola, J. M. delCampo, V. D. Domínguez-Soria, R. F. Moreno, G. U. Gamboa, A. Goursot, A. M. Köster, J. U. Reveles, T. Mineva, J. M. Vásquez-Pérez, A. Vela, B. Zúñinga-Gutierrez, D. R. Salahub, *Wiley Interdiscip. Rev.: Comput. Mol. Sci.*, **2**, 548 (2012).
17. J. P. Perdew, Y. Wang, *Phys. Rev. B*, **46**, 12947 (1992).
18. A. Goursot, T. Mineva, R. Kevorkyants, D. Talbi, *J. Chem. Theory Comput*., **3**, 755 (2007).
19. N. Godbout, D. R. Salahub, J. Andzelm, E. Wimmer, *Can. J. Chem*., **70**, 560 (1992).
20. J. C. Slater, *Phys. Rev*., **34**, 1293 (1929).
21. J. F. Janak, *Phys. Rev. B*, **18**, 7165 (1978).
22. A. Sachse, V. Hulea, K. L. Kostov, N. Marcotte, M. Y. Boltoeva, E. Belamie, B. Alonso, *Chem. Commun.*, **48**, 10648 (2012).
23. A. Sachse, V. Hulea, K. L. Kostov, E. Belamie, B. Alonso, *Catal. Sci. Technol*., **5**, 415 (2015).
24. A. Sachse, L. Cardoso, K. L. Kostov, C. Gerardin, E. Belamie, B. Alonso, *Chem. Eur. J*., **21**, 3206 (2015).
25. N. I. Petkova, R. D. Nikolova, K. L. Kostov, T. Mineva, G. N. Vayssilov, *J. Phys. Chem. A*, **118**, 11062 (2014).
26. E. Belamie, P. Davidson, M. M. Giraud-Guille, *J. Phys. Chem. B*, **108**, 14991 (2004).
27. B. Alonso, E. Belamie, *Angew. Chem. Int. Ed.*, **49**, 8201 (2010).
28. L.-S. Johansson, J. M. Campbell, *Surf. Interface Anal*., **36**, 1018 (2004).
29. S. Danielache, M. Mizumo, S. Shimada, K. Endo, T. Ida, K. Takaoka, E. Kurmaev, *Polymer Journal*, **37**, 21 (2005).
30. G. Beamson, D. Briggs, High Resolution XPS of Organic Polymers. The Scienta ESCA 3000 Database, John Wiley &Sons, Inc., Chichester, UK, 1992.
31. D. Carlstrom, *J. Biophysic. Biochem. Cyto*., **3**, 669 (1957).
32. Y. K. Gao, F. Traeger, O. Shekhah, H. Idriss, C. Woell, *J. Coll. Interface Science*, **338**, 16 (2009).
33. P. B. Dengis, P. A. Gerin, P. G. Rouxhet, *Colloids Surfaces B: Biointerfaces*, **4**, 199 (1995).
34. R. L. Graham, C. D. Bain, H. A. Biebuyck, P. E. Laibinis, G. M. Whitesides, *J. Phys. Chem*., **97**, 9456 (1993).

ХИМИЧЕСКИ СЪСТОЯНИЯ НА ПОВЪРХНОСТИТЕ НА ЦЕЛУЛОЗА, ХИТИН И ХИТОЗАН, ИЗСЛЕДВАНИ ЧРЕЗ ТЕОРИЯТА НА ФУНКЦИОНАЛА НА ПЛЪТНОСТТА И ФОТОЕЛЕКТРОННА СПЕКТРОСКОПИЯ С ВИСОКА РАЗДЕЛИТЕЛНА СПОСОБНОСТ

К. Л. Костов[1], Е. Белами[2, 3], Б. Алонсо[2], Ц. Минева[2]

[1] Институт по обща и неорганична химия, Българска академия на науките, 1113 София, България
[2] Институт Шарл Герар на Монпелие-Френски национален център за научни изследвания, Университет на Монпелие – Висше национално училище по химия на Монпелие, Авеню Проф. Емил Жанбро, 34090 Монпелие, Франция
[3] Практическо училище за висши науки, Изследователски университет, 75014 Париж, Франция

Постъпила март, 2018 г.; приета април, 2018 г.

(Резюме)

Комбиниран теоретичен и експериментален подход е приложен в изследването на електронните 1s енергетични свойства на повърхностите на целулоза, хитин, синтезирани хитинови нано-пръчки и хитозан, използвайки теорията на функционала на плътността и фотоелектронна спектроскопия с висока разделителна способност. Това позволява надеждно да се различат приносите на повърхностните въглеводородни замърсявания във фотоелектронните спектри и да се оцени в детайли химическите състояния на полизахаридните повърхности. Въпреки че е предположена стехиометрична структура на целулозната повърхност като най-вероятна, е разгледан и механизъм за възможна деградация на повърхността, включващ отстраняване на ОН-групата, свързана към глюкозения ринг. Доброто съответствие между теоретичните и експериментални резултати позволява да се предположи хитозан-подобна структура за повърхностите на хитина и хитиновите нанопръчки. В допълнение към доминиращата концентрация на амино NH_2 групи върху тези повърхности, се наблюдава и малко количество ацетил-аминови NH_2COCH_3 групи върху хитина. Възможно е присъствието на протонирани амино NH_3^+ функционални групи, вместо ацетил-аминови, върху кристалните повърхности на хитиновите нанопръчки. Дискутирана е и възможната деструктивна роля на рентгеновото облъчване върху изследваните повърхности.